SDA with the PTD-R and GEOstare SV2 Nano-Satellites

Willem de Vries
Lawrence Livermore National Laboratory, Space Program
Nathan Golovich, J. Luc Peterson, Phillip Rittmuller, Lance Simms, Jordan Smilo, Kelsey Tresemer, Peter Waswa
Lawrence Livermore National Laboratory, Space Program
Talin Guliani, Rishay Jain, Ziad Ramadan
Lawrence Livermore National Laboratory, Space Program and University of California, Berkeley
Emily Milne, Brendan Smith, Michael Higgins, Luis Andrade, Declan King, Courtney Melville, Ryan Downs, Shawn Joseph, Kyle Kung, Christopher Laurent
Terran Orbital Corporation

ABSTRACT SUMMARY

Lawrence Livermore National Laboratory (LLNL), in collaboration with NASA and commercial partner Terran Orbital, is currently supporting the operations of the Pathfinder Technology Demonstration Replacement (PTD-R) satellite, as well as our earlier GEOstare SV2 demonstrator satellite, launched in 2021[1]. Both are 6U CubeSats equipped with co-boresighted imaging channels. This presentation focuses on Space Domain Awareness (SDA) demonstrations using both satellites, as opposed to results for the individual satellites [1,2]. We imaged Geostationary Orbit (GEO) satellites simultaneously from both platforms, enabling range estimates through triangulation. The initial orbit determinations (IOD) in our reported example campaign are good enough to recover the resident space object (RSO) a few hours later within the field of view of GEOstare SV2. We also demonstrate the feasibility of these small imaging platforms to capture and track near-Earth asteroids, highlighting the agile tracking capabilities of these small platforms. Finally, as an enabling capability, we report on our automated tasking / scheduling and Unified Data Library (UDL) connectivity. This level of automation and integration into the larger SDA ecosystem shows that these small satellite platforms can provide a scalable approach to space-based SDA that is complementary to existing ground- and space-based capabilities.

1. INTRODUCTION

Lawrence Livermore National Laboratory (LLNL) have been developing monolithic optics technology since 2014, resulting in several nano-satellite demonstration missions in collaboration with our industry partner Terran Orbital Corporation under a collaborative R&D agreement (CRADA). This paper concerns with the 2 most recent missions. The first one, GEOstare SV2, was launched in May of 2021 and is still operational. A more detailed description of its capabilities and some SDA implications using advanced tracking modes are discussed in [1]. The second mission, Pathfinder Technology Demonstrator – Mission R (PTD-R) was launched in August of 2024. It is a joint satellite mission between LLNL, Terran Orbital, and NASA. A fuller description can be found in [2], but for the sake of convenience, we are summarizing the most relevant aspects of both missions in the next paragraph.

Both SV2 and PTD-R are 6U nano-satellites built by Terran Orbital. They are very similar in size and configuration, though SV2 has 2 hinged solar panels, versus one slightly larger one for PTD-R. The telescopes for the imaging payloads provided by LLNL are based on monolithic optics technology, see Fig. 1. The SV2 mission was designed for day-time ISR (Intelligence, Surveillance, and Reconnaissance) imaging experimentation, while the local nights are used for SDA campaigns. As such, it carries a diffraction-limited 85mm diameter F/7.6 narrow field-of-view channel for ISR, and a wide-field 85mm diameter telescope with a 306mm focal length (F/3.6) for SDA. Both sensors are operating in the optical regime (0.4 – 0.9 micron). We used the wide-field telescope for the SV2 SDA results shown in this paper. PTD-R uses two identical 85mm telescopes for its imaging channels, both wide-field options similar to the SV2 wide-field channel (F/3.6). However, unlike SV2 that operates exclusively in the optical,

PTD-R uses a narrow UV channel (0.26-0.31 micron), as well as a Short Wave IR (SWIR) sensor with a spectral response across 0.93 – 1.7 micron. See [2] for more details.

The outline of the paper is as follows. Section 2 describes results from our recent stereo-imaging campaign where both spacecraft were targeting the same GEO satellite at the same time (or as near as possible). Section 3 showcases target tracking results on a challenging flyby of a near-Earth asteroid, and the use of photometric data in combination with good temporal coverage allowing for an estimate of its rotational period. In Section 4, we go into ongoing efforts to automate SDA tasking of our nano-satellites, and linking up with the Unified Data Library (UDL) through experimentation with the MACHINA framework [7].

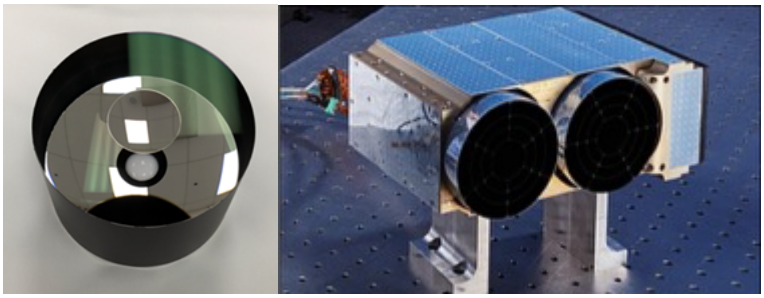

Fig. 1. Left panel: Monolithic Cassegrain telescope design as used in SV2 and PTD-R. All apertures are 85mm in diameter. Right panel: co-boresighted payload setup with both telescopes looking in the same direction.

2. STEREO IMAGING CAMPAIGN

Our observations with the on-orbit platforms are angles-only, i.e., we do not extract range information from the collects, just a relative look angle. Examples of the pipeline processed collects for SV2 and PTD-R are shown in Figs. 2 and 3, respectively. This astrometric pipeline was designed to run on the spacecraft locally to reduce data volume, but for our normal experimentation runs, we were not bandwidth limited and therefore downloaded the full captured image sequence.

In order to get a decent initial orbit determination (IOD) for RSOs in the GEO regime, one would typically have to collect angles-only imagery over a significant fraction of the RSO's orbit. This could amount to several hours, and if more or less continuous coverage is not available, maneuvering RSOs might get lost. If one, on the other hand, would use 2 (or more ideally) dispersed imaging platforms to look at the same region of GEO at the same time, one could use regular triangulation approaches to get a handle on range as well. With the recent tasking upgrades to PTD-R (see Section 4), we were able to schedule a few of these stereo campaigns near the end of July 2025. In this paragraph, we are going to discuss our campaign against 56370 VIASAT 3-F1, a large geostationary communications satellite.

As it would happen, it was not near the predicted TLE position. Figs. 2 and 3 show the expected position of VIASAT as seen from the vantage point of the satellite, and it is clear from both viewpoints that it is, or has been, undergoing a small maneuver. Other satellites in the field-of-view (particularly of SV2's larger FOV) are detected at the expected positions. The VIASAT observations therefore provide an excellent opportunity to see whether triangulation can improve IOD estimates with particularly short orbital arcs. Table 1 lists the pipeline processed metric observations for both platforms. Unlike SV2 that can execute exposures at fixed times, PTD-R takes them in series as quickly as the system will allow. This means that the observations are not exactly at the same time, but are coincident within a fraction of a second typically. To match the SV2 results to the PTD-R timestamps, we interpolated the RA, Dec pairs for the former platform so that we can start to determine the triangulation results listed in Table 2.

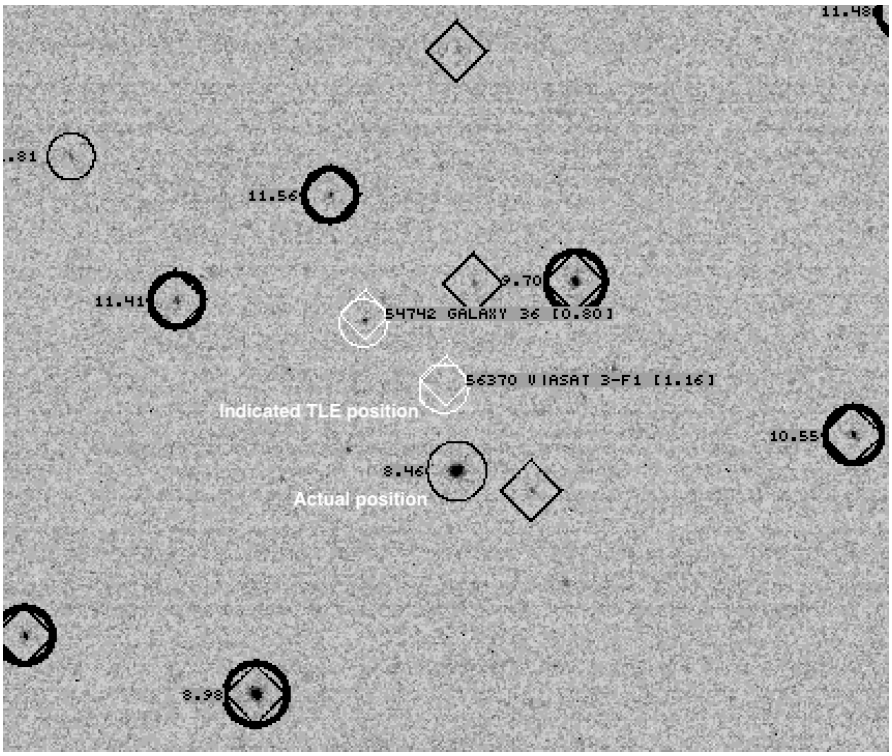

Fig 2. Cropped image taken by GEOstare SV2 of 56370 VIASAT. Note the slightly stale TLE (1.16 days old) predicting a different position compared to the actual observed one. The agreement for 54742 GALAXY 36 is much better. Catalog stars are surrounded by a tilted square, with ones selected for astrometric purposes marked with a bold circle. Image taken on July 26 2025 at 06:24:57.3s UTC.

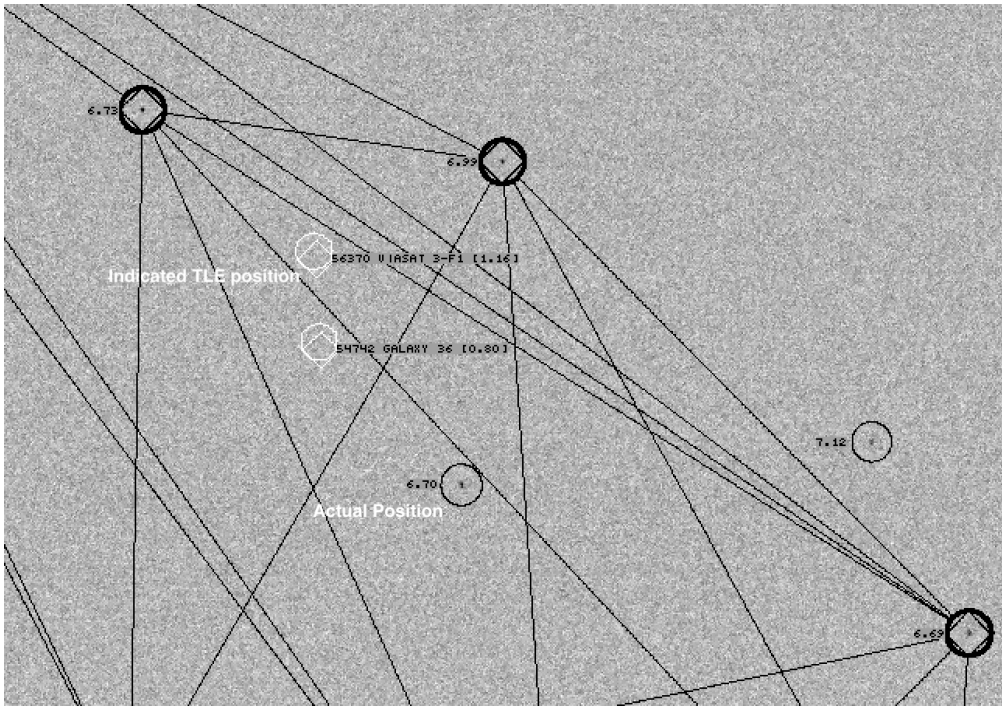

Fig. 3. Cropped image from PTD-R, using the SWIR channel. The offset between indicated and actual positions for 56370 VIASAT are obvious, though from a different perspective compared to Fig. 2. The other RSO, 54742 GALAXY 36 is too dim for the SWIR channel, but does show up very close to the indicated position in Fig. 2. Image taken on July 26, 2025 at 06:24:55.0s UTC.

#	JD	Date/Time UTC	Spacecraft	RA (J2000)	Dec (J2000)	Magnitude
1	2460882.76726000	06:24:51.264	SV2	319.01113	-4.08726	8.40 C
2	2460882.76727942	06:24:52.942	PTD-R	312.02779	8.47090	6.62 H
3	2460882.76728314	06:24:53.264	SV2	319.02020	-4.07282	8.51 C
4	2460882.76728526	06:24:53.447	PTD-R	312.03239	8.46866	6.70 H
5	2460882.76729109	06:24:53.951	PTD-R	312.03713	8.46642	6.66 H
6	2460882.76729693	06:24:54.455	PTD-R	312.04143	8.46445	6.66 H
7	2460882.76730276	06:24:54.959	PTD-R	312.04621	8.46198	6.48 H
8	2460882.76730628	06:24:55.263	SV2	319.0290	-4.05850	8.48 C
9	2460882.76732026	06:24:56.471	PTD-R	312.06037	8.45559	6.50 H
10	2460882.76732611	06:24:56.976	PTD-R	312.06441	8.45342	6.52 H
11	2460882.76732943	06:24:57.263	SV2	319.03792	-4.04380	8.52 C
12	2460882.83531557	08:02:51.266	SV2	344.80645	-2.36033	9.14 C
13	2460882.83532968	08:02:52.485	PTD-R	340.60422	6.57042	7.19 H
14	2460882.83533552	08:02:52.989	PTD-R	340.60913	6.56693	7.33 H
15	2460882.83533872	08:02:53.266	SV2	344.81708	-2.34429	9.17 C
16	2460882.83536187	08:02:55.266	SV2	344.82783	-2.32849	9.18 C
17	2460882.83538502	08:02:57.266	SV2	344.83853	-2.31259	9.10 C

Table 1. Metric observation log of PTD-R and SV2 targeting 56370 VIASAT 3-F1. The RA and Dec values are in decimal degrees; the listed magnitudes are estimates based on calibration using field stars. C and H stand for Clear and H-band magnitude, respectively.

#	JD	ECI x coord [m]	ECI y coord [m]	ECI z coord [m]
1	2460882.76727942	2.7607296e+07	-3.1330600e+07	-7.6254222e+02
2	2460882.76728526	2.7608241e+07	-3.1329383e+07	-7.6398500e+02
3	2460882.76729109	2.7609341e+07	-3.1328267e+07	-7.6737865e+02
4	2460882.76729693	2.7609448e+07	-3.1326394e+07	-7.2488211e+02
5	2460882.76730276	2.7610962e+07	-3.1325659e+07	-7.8275437e+02
6	2460882.76732026	2.7613896e+07	-3.1321986e+07	-6.1337348e+02
7	2460882.76732611	2.7614122e+07	-3.1320346e+07	-5.9233794e+02
8	2460882.83532968	3.7700330e+07	-1.6916313e+07	2.4288334e+03
9	2460882.83533552	3.7697262e+07	-1.6914082e+07	2.4893445e+03

Table 2. Position vectors for 53760 VIASAT derived from direct triangulation of the results in Table 1. The epoch of the vector is the current one (i.e., as listed by the JD column). These vectors are used to derive the TLEs listed in Table 3.

Since the RA, Dec pairs are reported out by the astrometric pipeline in the J2000 epoch, care has to be taken to precess it back to the actual observed epochs. This makes sure that the reported TLE positions and the look vectors are in the same epoch, and that we can use the spacecraft position vectors and the look vectors for proper triangulation. Table 2 lists the results for the PTD-R timestamps. It should be noted that the triangulation vectors do not intersect, but have a “closest approach” near the VIASAT location. We used the middle position of both closest points on the triangulation vectors to estimate the VIASAT position. Given the rather large range to GEO, typical closest approach distances are on the order of 70km.

Data range	Derived TLE with *e, i* constraints
4.0 seconds (#1-7)	0 VIASAT_SHORTARC_A_4S 1 99999U 25001A 25207.26730026 .00000000 00000-0 00000-0 0 0006 2 99999 0.0136 315.5234 0009971 359.4104 356.4659 1.01591505 05
98 minutes (#1-9)	0 VIASAT_SHORTARC_B_96M 1 99998U 25001A 25207.28241856 .00000000 00000-0 00000-0 0 0007 2 99998 0.0100 319.5785 0000001 1.4382 355.8083 1.01943145 03

Table 3. TLEs generated using vectors from Table 2, and e<0.01 and i<0.02 constraints

The position vectors in Table 2 allow us to use either the first 7 data points for a 4 second orbital arc, or all 9 data points to add 2 more observations at +96 minutes. If we fit the 4-second are without any priors, the best fitting orbit has very small errors (x,y,z, residual fitting uncertainties of 0.29, 0.21, and 0.02 km) but clearly is not very useful with its eccentricity of 0.23. The arc is just too short. However, if we make assumptions about the RSO (we were targeting GEO to begin with), and introduce inclination and eccentricity limits to both less than 0.01, we get orbits that are not nearly fitting as well but turn out to be useful. They are listed as TLEs in Table 3.

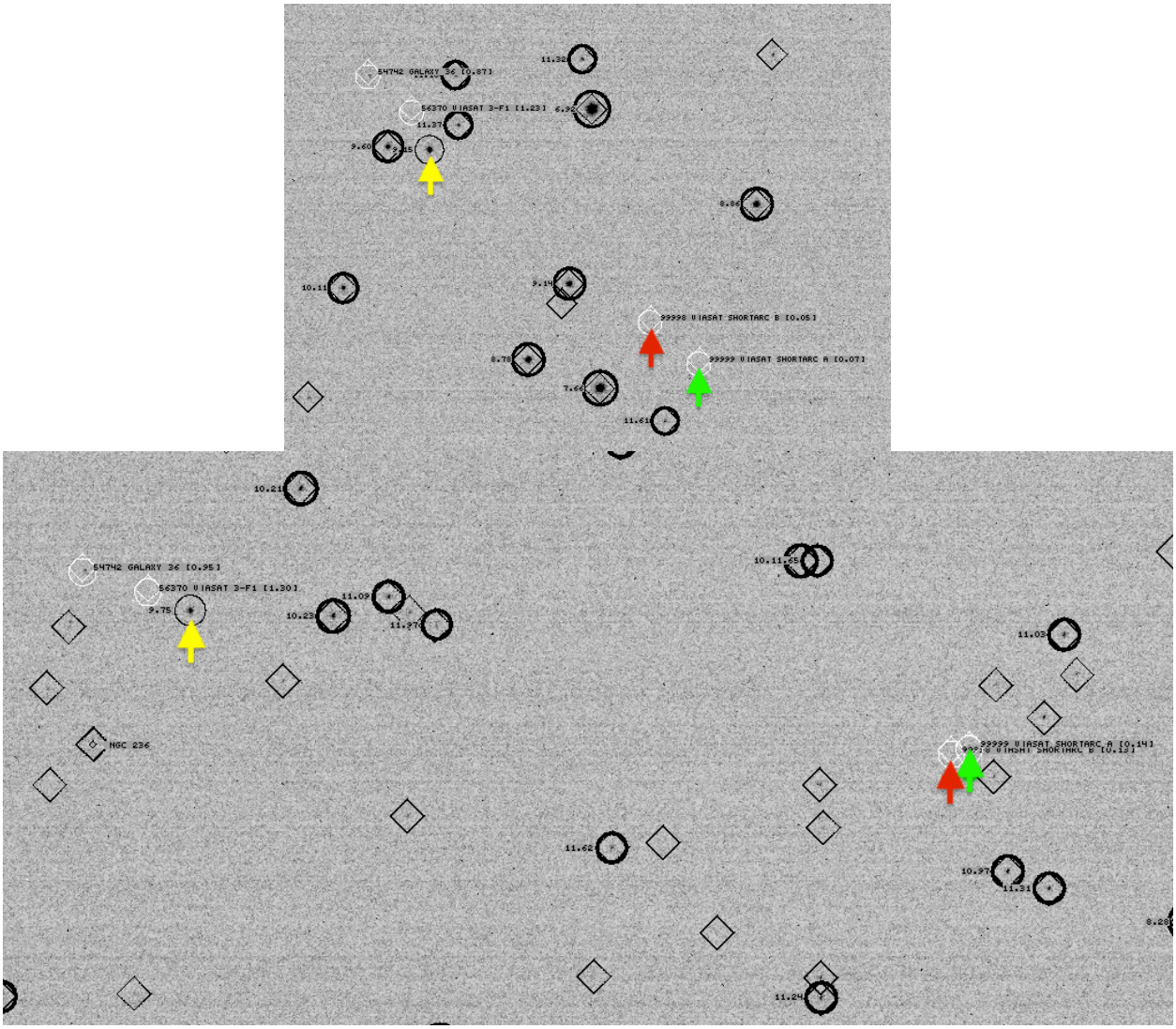

Fig. 4. Extremely short-arc- (4s, labelled as SHORTARC_A, green arrow) and longer 96m-based (SHORTARC_B, red arrow) predicted VIASAT positions versus actual (yellow arrow) as observed by SV2 96 minutes (top) and 203 minutes (bottom) later. Note that both images are small cut-outs of the full SV2 FOV.

It turns out that both IODs can be used to recover the moving RSO within a few hours, provided the FOV of the sensor is large enough. SV2's wide field has a diagonal of 2.5 degrees. Fig. 4 shows the quality of the IOD against actual images, and Table 4 lists the results as angular offsets. In summary, while neither of these IODs are particularly accurate (especially the 4 arc), they can serve a purpose to keep custody of maneuvering RSOs. Stereo imaging of GEO (or near GEO objects) from multiple platforms can provide accurate enough ranging information that improved IOD estimates considerably.

Time since IOD	SHORTARC_A 4s	SHORTARC_B 96 min	Actual VIASAT TLE
0 s	0.03 degrees	0.14 degrees	0.05 degrees
96 minutes	0.37 degrees	0.30 degrees	0.05 degrees
203 minutes	0.77 degrees	0.75 degrees	0.05 degrees

Table 4. IOD accuracy results, listed as angular separation between observed and indicated positions.

3. NEAR-EARTH ASTEROID TRACKING

As described in [1], we have implemented advanced tracking algorithms in both of our nano-satellites. In this paragraph, we highlight the result of one of our recent Near-Earth Object (NEO) asteroid flyby tracking campaigns. By using predicted ephemeri from the NASA Jet Propulsion Laboratory (JPL) Center for Near Earth Object Studies[3], we were able to use target-tracking mode as opposed to inertial guiding combined with a shift-and-add post-processing step to elevate the low-significance detections above a meaningful threshold.
Our particular example in this paper concerns the NEO 2005-LW3, a potentially hazardous asteroid with a 630 day Earth crossing orbit[4,5], and an estimated size of 200-300 meters. We collected 49 multi-exposure sessions over a period of almost 2 days with GEOstare SV2 around its closest approach to the Earth around November 23, 2022.

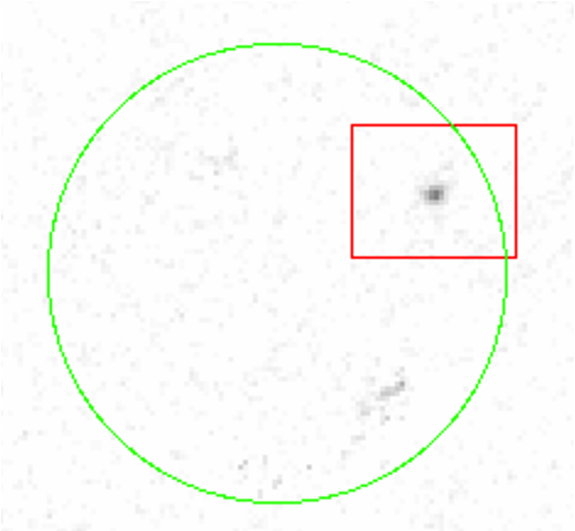

Fig. 5. NEO asteroid 2005 LW3 as tracked by SV2. The observed position (red box) was close to the expected position (center of green circle).

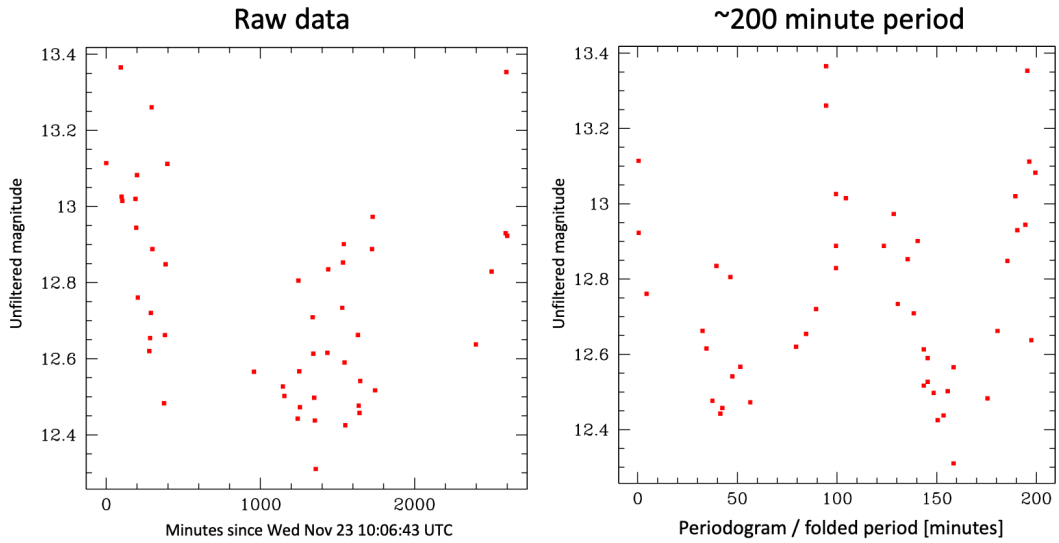

Fig.6. Raw photometric data collected over almost 2 days (left panel, unfiltered magnitudes), and the best fitting folded period estimate of about 200 minutes (3.3 hours), not too far off from the radar measurements of 3.6 hours [6]. The accuracy of each photometric measurement is about 0.1 magnitude.

As can be seen in Fig. 5, even though the NEO was not particularly nearby (closest approach was about 1.1 million km, or about 3 Lunar distances [5]), by tracking on the target, the stars are trailing noticeably during each collection window. The collected photometry is presented in Fig. 6, left panel. Since the photometric solutions on the unfiltered CMOS sensor of SV2 are calibrated using UCAC-4 R-band photometry, we consider the reported magnitudes to be not particularly accurate, with error-bars estimated on the order of 0.10 magnitudes. We have left these off the plot for clarity purposes. However, even though these measurements are not very accurate, they can be used to estimate the rotational period of the asteroid. Our best guess, using an appropriate period folding, is about 200 minutes, or 3.3 hours. This is remarkably close to 3.6 hours based on detailed radar observations [6], underlining the utility that can be had from very modest apertures from space. This particular flyby provided additional acquisition opportunities from our space-based platform not available to ground-based observatories.

4. AUTOMATED TASKING AND UDL CONNECTIVITY

4.1 Introduction

Space Domain Awareness (SDA) demands rapid, high-volume imagery in response to radar and optical detections. Relying on manual satellite tasking creates significant bottlenecks in the observe-analyze-act cycle, which is critical for both space and national security operations.

To address these limitations, we developed an automated software pipeline that enables decision-makers to access and task LLNL satellites, turning ground-based observations into executable satellite commands. This system streamlines the connection between initial detections and satellite operations without the delays inherent to manual scheduling, yielding greater imaging frequency with lower time overheads. Automatic tasking of SDA sensors (both ground-based and space-based) is becoming increasingly common. For our assets, both PTD-R and GEOstare SV2, we have developed an autonomous scheduling and tasking system that is compatible with the MACHINA agent-based framework [7]. MACHINA allows for an extensible network of ground-based sensors to act as agents that can collectively coordinate their observations through a centralized asynchronous scheduler. In this work, we develop an automated scheduling system for space-based assets that is compatible with the MACHINA ecosystem. While developed for our LLNL satellites, the system is generic and extensible to any space-based sensor, augmenting MACHINA's capabilities to now include coordinated ground-and-space observations.

Data and processing are conducted at the LLNL Satellite, Telescope, Aerial drone and Remote sensing Mission Operations Center (STARMOC). New observation requests posted by MACHINA to the Unified Data Library (UDL) [8] are pulled and processed by an agent running at the STARMOC into valid observation instructions to the satellite. These are sent to Terran Orbital for uploading by a human-in-the-loop operator. After observations are downlinked, the same human-in-the-loop vets the observations and posts them to a central repository, where the STARMOC agent can see them and process them into valid observations for re-posting to the UDL and MACHINA. In the future, this system could be extended to enable fully autonomous or human-on-the-loop operations, with full machine-to-machine connections and a human monitoring communications for risk reduction.

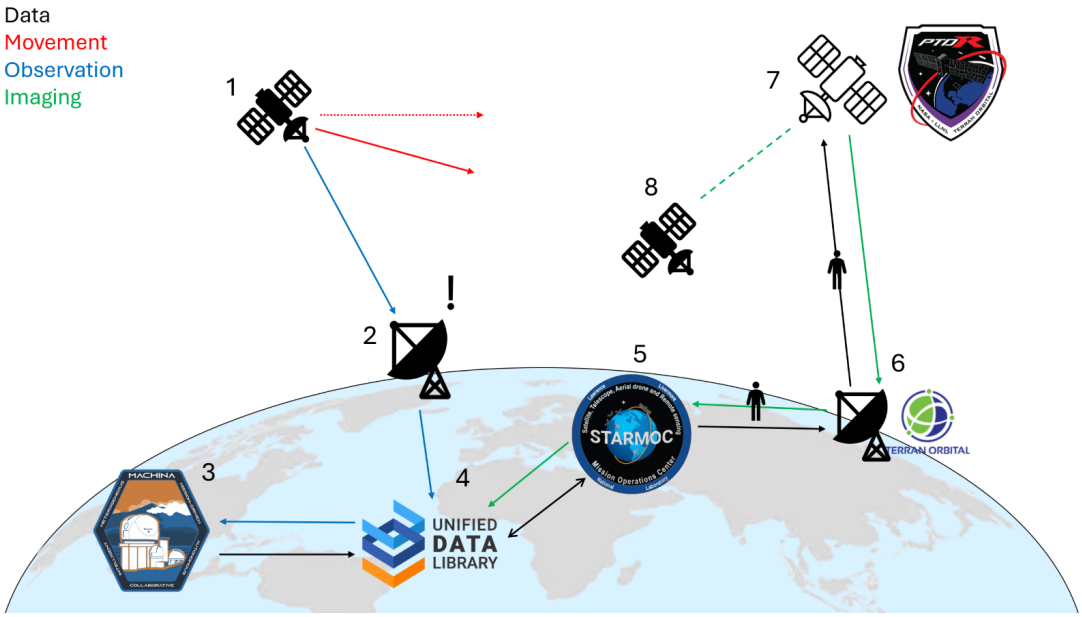

Fig. 7. System diagram for the coordination and tasking of space-assets with MACHINA. Collection requests are orchestrated by MACHINA with data and messages passing via the Unified Data Library (UDL). The LLNL Satellite, Telescope, Aerial drone and Remote sensing Mission Operations Center (STARMOC) automatically pulls new requests from the UDL, translates the requests to satellite-specific commands and sends them to Terran Orbital for upload to the satellites. When observations are received, vetted, and placed in a central repository, algorithms at the STARMOC pull the data, process it, extract necessary observation data and post the data back to the UDL and MACHINA.

Fig.7 shows the system design of the current semi-automated system for the tasking of PTD-R. When a satellite has deviated off-course from its predicted orbit (1 – numbers refer to labelling in Fig. 7) more information is required to find its new orbit. When a ground station observes the change in the predicted orbit (2) an observation is made and sent to the Unified Data Library (UDL) (4). That observation is then ingested by MACHINA (3) who then task a sensor to take an observation of the satellite at a new projected position (8). A command request is then sent to the UDL (4). If that command request asks for PTD-R (7) to take an image, the collect request is ingested to the STARMOC (5) where scheduling is done in order to create a command template to tell PTD-R (7) when to take an image, where to look to take an image, and the specifics of the images such as quantity and exposure time. That is then sent to our partners at Terran Orbital (6) who have a person check our command templates before they are then sent to PTD-R (7) to take an image of the target satellite (8). Once the image is taken by PTD-R (7), it is sent to Terran Orbital (6), and then retrieved at the STARMOC (5) with human intervention. Once the images arrive at the STARMOC (5), those images, their metadata, and where they are pointing in the sky are all uploaded to the UDL (4).

4.2 Technical details of the pipeline

The UDL allows for the posting of CollectRequests in the form of a JSON structure that can be queried and fetched via their REST API. Each request contains information about its creator, requested sensor, and target information. Although built with integration into MACHINA in mind, our data processing and tasking pipeline is agnostic to the source of the CollectRequest. Most CollectRequest creators will supply an observation (state vector) of a target at some earlier instant in time. In this case, LLNL's STARMOC pipeline will independently propagate its position and calculate the optimal viewing opportunity for an LLNL satellite. Alternatively, our pipeline can handle requests that already come with the optimal time pre-calculated, as MACHINA does for its orchestration. These requests, which have already been calculated based on the position of PTD-R, do not need to be fully scheduled by STARMOC; instead, the pipeline checks to ensure constraints (e.g., acceptable Sun-target angle) have been met and the calculated state vector is within an acceptable tolerance of STARMOC's own calculation.

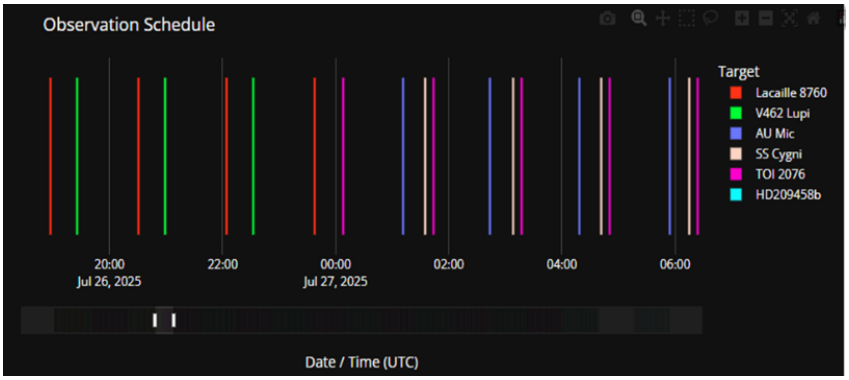

Fig. 8. A main satellite schedule is kept in a centralized database to ensure new requests are permissible.

Once a viewing opportunity has been identified, the STARMOC pipeline checks the timeslot against a running mission schedule, which collects all scheduled tasks for a satellite (Fig. 8). If the timeslot is open (or the existing event is of a lower priority), the new request is slotted in. This opportunity is then used to create a JSON command with the relevant information for the target and imaging satellite, which is automatically communicated to operations partners at Terran Orbital Corporation.

4.3 Adaptability across satellites

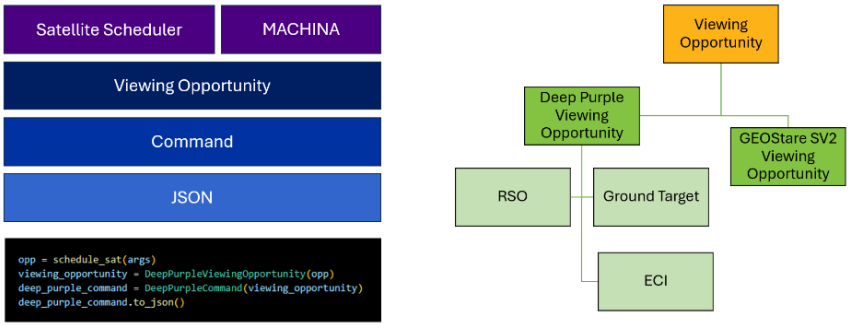

Fig. 9. Layout of STARMOC pipeline

The STARMOC pipeline (Fig. 9) establishes internal schemas that collect the requirements for a 'Viewing Opportunity' and 'Command'; these are extended to form mission-specific objects, such as 'DeepPurpleCommand'

for PTD-R, which hold the tasking information along with satellite-specific imaging modes and command templates. The handling of data through these abstractions makes it ultimately possible to perform multi-satellite operations, including the possibility of synchronizing/sharing viewing opportunities between satellites.

4.4 Example results

Metric	Previous approach	Updated approach
Request to Command	~15 minutes (manual)	16 seconds (automatic)
Daily Throughput	~25 image sessions scheduled	700 sessions (7/23/25) scheduled

Table 5. Metrics gathered from timed testing and realized performance

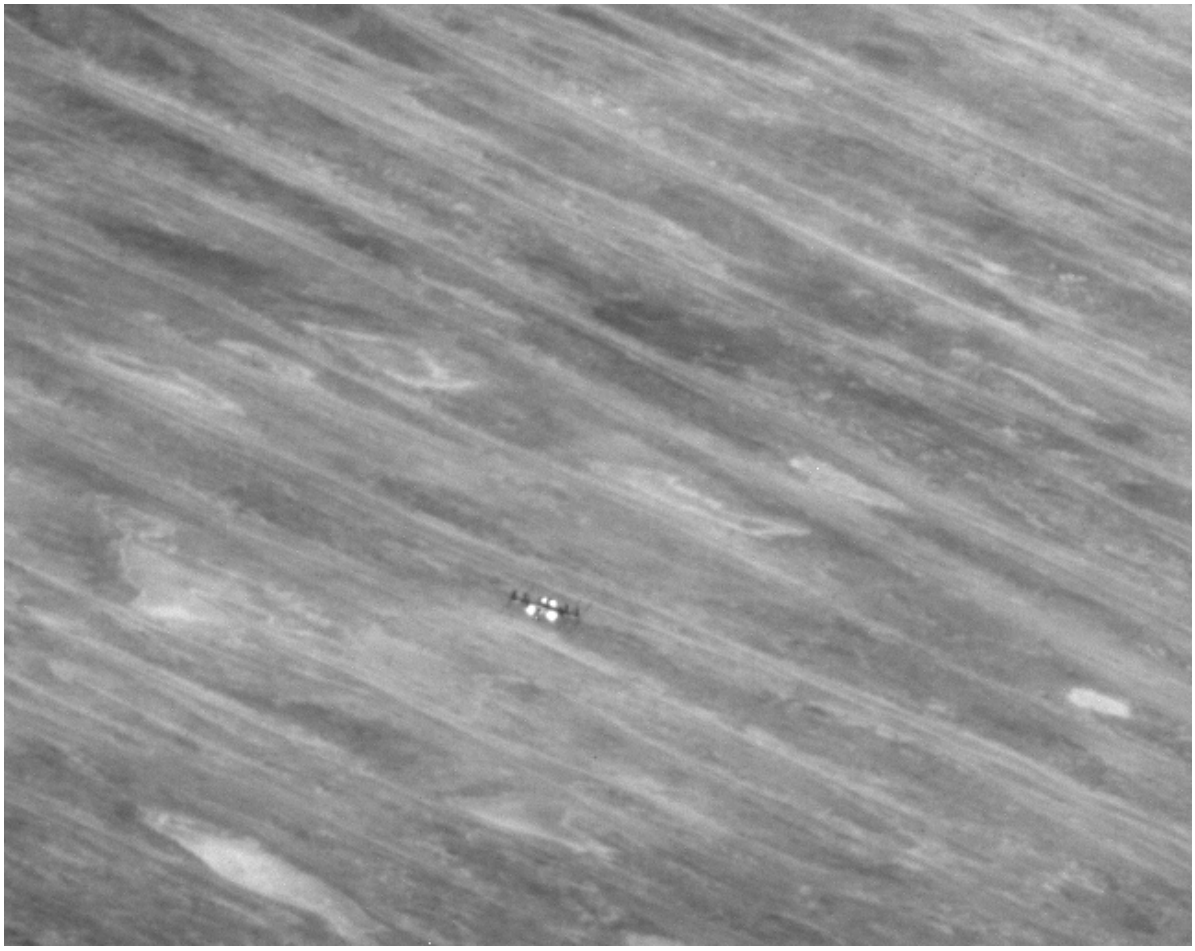

Fig. 10. Image of the ISS taken by PTD-R using the MACHINA to LLNL pipeline.

As shown in Table 5, our implementation with PTD-R has demonstrated improvements in operational capabilities; in testing, our system reduced scheduling lead time by several orders of magnitude, significantly increased daily imaging throughput, and enabled new modes of operation (e.g., 'Periodic Revisits' of ECI targets) that were previously impractical due to manual scheduling constraints. By automating the observe-act feedback cycle, our system enables the rapid characterization of targets in space. Fig. 10 shows ISS being captured by PTD-R as an example of automated scheduling, while also showcasing the pointing and timing accuracies of the nano-satellite.

5. SUMMARY

We demonstrate the utility of small imaging satellites for SDA applications. In particular, the simultaneous observations of RSOs from spatially separated satellites adds to the tracking capabilities of the system as a whole. Obtaining range information through triangulation can improve the timeliness of orbit estimates dramatically, and it is likely that a larger constellation of similarly capable nano-satellites can contribute meaningfully to the SDA enterprise. It is in this context that the reported automation and level of tasking integration with UDL is especially relevant.

6. ACKNOWLEDGMENTS

This work was performed under the auspices of the U.S. Department of Energy by Lawrence Livermore National Laboratory under Contract DE-AC52-07NA27344 with document number LLNL-CONF-2010754. NASA's Small Spacecraft & Distributed Systems program within the Space Technology Mission Directorate manages the PTD-R mission. The program provided funding for the PTD-R spacecraft, launch, and mission operations through February 2025. We are very thankful for support from the United States Space Force, who provided funding for spacecraft operations for PTD-R from March 01, 2025 onwards.

We also recognize the excellent work and technical results provided by the summer interns to LLNL's Space program.

7. REFERENCES

[1] A Pertica, W de Vries, et al., Proceedings of the Advanced Maui Optical and Space Surveillance (AMOS) Technologies Conference, 2023
[2] L Simms, J Smilo, et al., SmallSat conference, 2025, Salt Lake City, UT
[3] Center for Near Earth Object Studies, NASA JPL, http://cneos.jpl.nasa.gov/ca/
[4] https://www.spacereference.org/asteroid/2005-lw3
[5] D Farnocchia, V Reddy, et al. The Planetary Science Journal, volume 4, 203
[6] Central Bureau for Astronomical Telegrams, 2022, December 10, telegram number 5198
[7] J. R. Fletcher, J. E. Kadan, "Autonomous interactive agents for global telescope network orchestration," Proc. SPIE 13101, Software and Cyberinfrastructure for Astronomy VIII, 131012U (25 July 2024); https://doi.org/10.1117/12.3018554
[8] Unified Data Library *https://unifieddatalibrary.com/* (Retrieved Aug 21, 2025)